The Grain Size Dependence on Diffusion Bonding Behavior in Superplastic Mg Alloys

Hidetoshi Somekawa[1,*], Hiroyuki Watanabe[2] and Kenji Higashi[1]

[1]*Department of Metallurgy and Materials Science, Osaka Prefecture University, Sakai 599-8531, Japan*
[2]*Mechanical Engineering Department, Osaka Municipal Technical Research Institute, Osaka 536-8553, Japan*

Applicability of the diffusion bonding was examined in a superplastic magnesium alloy, AZ31, on two different grain sizes of 28 and 11 µm. In order to investigate the superplastic behavior, the tensile test was carried out at the strain rates from 10^{-4} to $10^{-2}\,\mathrm{s}^{-1}$ at elevated temperatures. These materials showed a superplastic behavior at 673 K. The diffusion bonding tests were carried out in the superplastic region, which is the pressure range from 2 to 10 MPa and for the times up to 10 h at 673 K in air. The post-bonded mechanical properties were estimated by the compression lap shear test in order to determine the optimal diffusion bonding conditions. The diffusion bonded specimens exhibited more than 0.8 of parent material strength at several conditions for both materials. The bonding time on fine grained AZ31 could achieve much faster than that on coarse grained AZ31. Using this result, the comparison was carried out experimental results and previous theoretical diffusion bonding models. Many researchers constructed the theoretical models based on the void growth mechanism, diffusional controlled process, to predict its optimal bonding time and pressure. However, the previous modes were not agreement with experimental result. It was resulted from the previous models include only diffusional controlled process. Therefore, in this study, we developed new theoretical diffusion bonding model both diffusional and plastic controlled processes. From the comparison, this model was good agreement with experimental. Using the theoretical diffusion bonding model and experimental results, the prediction map for high quality diffusion bonding of the superplastic magnesium alloys was suggested.

1. Introduction

Magnesium alloys are attracting great attention as the ecological point of view, since magnesium alloys are the lightest of all structural alloys. Furthermore, magnesium alloys have several good characteristics: high specific strength and stiffness, superior damping capacity, high thermal conductivity, high dimensional stability, good electromagnetic shielding characteristics and good machin-ability.[1] Despite these advantages, magnesium normally exhibits limited ductility because of hcp structure. Therefore, most magnesium products have been fabricated by casting, in particular, die casting. These technologies enable mass production of small components such as mobile phones, note book computer cases, and automotive components for instrument panels.[2] However, in general, wrought magne-sium alloys can be seen to have a higher strength and ductility than cast magnesium alloys. This primarily results from the fact that the grain size of wrought magnesium alloys is normally finer than that of cast magnesium alloys.[3] In order to exploit the benefits of magnesium alloys, it is important to develop the secondary process, which can effectively produce complex engineering components directly from the wrought products. Superplastic forming is generally a viable technique to fabricate hard-to-form materials into complex shapes. Superplastic forming (SPF) is often combined with the diffusion bonding (DB) in the manufacture.[4] The concurrent application of SPF and DB (SPF/DB) has been recognized as a novel manufacturing technology that can result in both cost reduction and weight saving compared with the conventional manufacturing method.[5,6]

Diffusion bonding is one of the joining techniques, and is a solid state joining process in which two clean metallic surfaces are brought into contact at elevated temperature, $<0.7T_m$, under a low pressure, where T_m is the absolute melting point of the material. There are several advantages in the diffusion bonding: low distortion, without fusion process, post weld joining, large joining area, dissimilar material bonding and so on.[7,8] In addition, there is the possibility of combining SPF/DB to manufacture complex sheet structures with reduced weight and fabrication costs compared with mechanically fastened structure. Therefore, superplastic titanium alloys have been widely used to SPF/DB in aerospace industry.[9,10] Despite these advantages, there are still several factors relating to diffusion bonding quality. In order to produce sound joining, it is important to examine the diffusion bonding conditions such as pressure, time and temperature. In the previous investigations, these external factors have been obtained using superplastic titanium alloys,[9–12] superplastic aluminum alloys,[13–15] superplastic magnesium alloys[16,17] and superplastic steels.[18,19] How-ever, it is not always the case that the only external factors such as pressure and temperature would affect diffusion bonding quality. In general, the superplastic high temperature deformation mechanism has grain size dependence in the tensile state. It is considered that the affection of structural factors might also exist in case of diffusion bonding.

In the present study, the superplastic behavior of com-mercial wrought AZ31 magnesium alloy sheets was exam-ined. The possibility to joint them by using diffusion bonding technique was demonstrated. Diffusion bonding tests were carried out in the wide range of bonding pressures and time to obtain its optimal conditions, in particular, the effect of the grain size on the diffusion bonding was evaluated. In

---

*Graduate Student, Osaka Prefecture University.

addition, the relationship between the bonding time and the grain size to form high quality diffusion bonding was clarified at several superplastic conditions.

2. Experimental Procedures

The material used in the present study was a sheet of Mg–Al–Zn alloy, AZ31, since which was one of the most popular wrought magnesium alloys. Two materials with different grain sizes were prepared. The typical optical microstructures after annealing at 673 K for 1.8 ks are shown in Fig. 1; (a) fine-grained and (b) coarse-grained materials. The measured grain sizes were 11 μm and 28 μm. The average grain sizes, d, were calculated using the equation, $d = 1.74L$, where L is the linear intercept size.

In order to investigate the superplastic behavior, the strain rate change tests were carried out at strain rate ranging from 10^{-4} to 10^{-2} s^{-1} at temperatures of 473, 573 and 673 K in air. Tensile specimens were machined from the annealed sheet at 673 K for 1.8 ks. They had a gauge length of 18 mm and a width of 6 mm, respectively. The specimens for the diffusion bonding were also cut directly from the annealed sheet with a length of 30 mm and a width of 20 mm, respectively. Before diffusion bonding, the bonded surfaces were blasted by using 20 μm diameter alumina particle in order to supply the rugged surface. It has been reported that this technique is

Fig. 1   The typical microstructure for (a) fine-grained AZ31 and (b) coarse-grained AZ31. The specimen was annealed at 673 K for 1.8 ks.

Table 1   Roughness dimensions of as-received and grit blasting treated surfaces.

	as-received	grit blasted
	$r'/$μm	$r'/$μm
fine grained AZ31	1.7	25.4
coarse grained AZ31	2.8	24.5

effective to remove the surface oxides and obtains higher quality in diffusion bonding.[7,14,20] The surface roughnesses of as-received and grit blasted materials are listed in Table 1. It was clearly found that these surface roughnesses were nearly equal to the particle size used for grit blasting treatment. After the specimens were cleaned in ethanol using ultrasonic vibration cleaner, the diffusion bonding tests were carried out at the bonding pressure ranging from 2.0 to 10 MPa at temperature of 673 K. The bonding time was up to 10 h in air.

Diffusion bonding quality was assessed by the compressive lap shear tests, because the specimens having different diffusion bonding conditions would have different mechanical properties. The compressive lap shear tests were carried out at cross-head speed of 5 mm/min at room temperature. The shear fracture strengths of the bonds were assessed by comparison with experimentally measured value for the parent metal, i.e. τ_b/τ_p, where τ_b and τ_p are the compression lap shear strength of the bond and the compression lap shear strength of the parent metal, respectively. Each of lap shear strengths was calculated by using follow equation.

$$\tau_p, \tau_b = P_{max}/(L \times 20) \qquad (1)$$

where P_{max} is the maximum load value and L is the diameter to be obtained P_{max}. Each of parent metal strengths, τ_p, was 89.1 (fine-grained) and 85.1 MPa (coarse-grained), respectively.

3. Results and Discussion

3.1 Superplastic behavior

It is known that the high strain rate sensitivity of flow stress is one of the important characteristics for superplastic deformation. In order to characterize the effect of strain rate of plastic flow behavior, the variation in flow stress as a function of strain rate was plotted in Fig. 2. It indicated that the flow stress increased with the strain rate. The strain rate sensitivity exponent, m, was estimated from the slope of the curve. It was found that m-value was in the low strain rate range increased with temperature. The m-value was calculated to be 0.5 for both fine-grained and coarse-grained materials in the low strain rate range at the temperature of 673 K. This high m-value of 0.5 suggested that grain boundary sliding could be a dominant deformation process.[21,22] From tensile results, it was found that the present used materials behaved in the superplastic manner at the temperature of 673 K.

The constitutive equation for the present materials in the superplastic region was also considered, because strain rate of the matrix, $\dot{\varepsilon}$, influences the diffusion bonding behavior as shown later. The constitutive equation to describe the superplastic flow can be generally expressed as,[23]
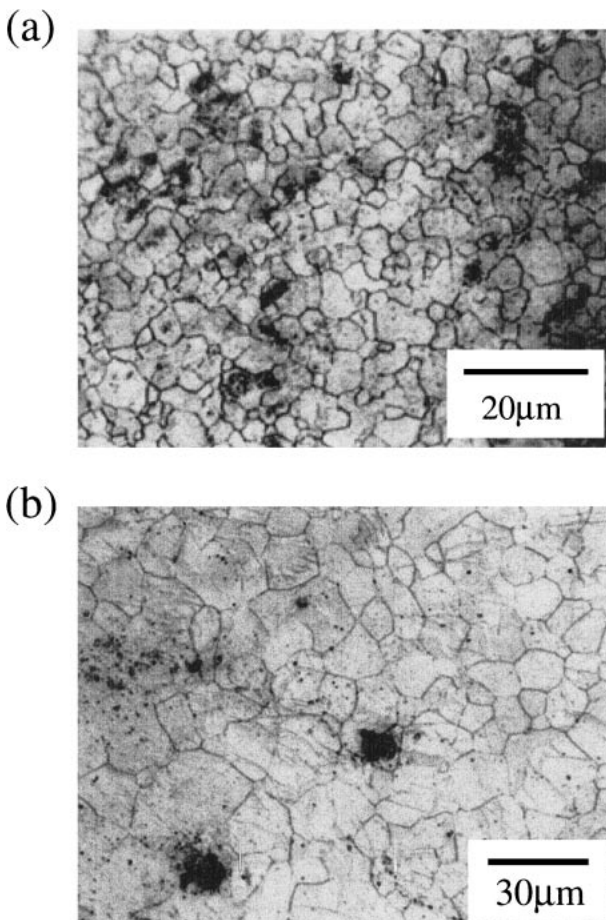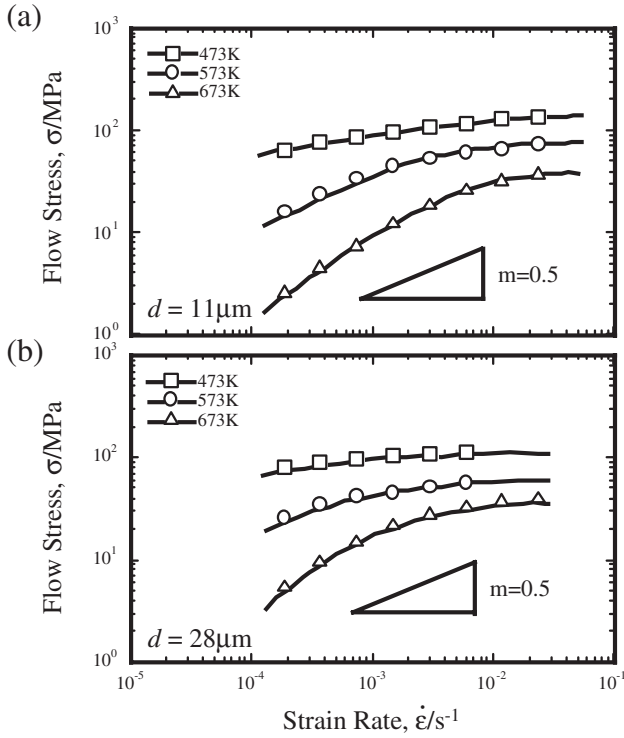
(a)

(b)

Fig. 2 Variation in flow stress as a function of strain rate at temperature of 673 K for (a) coarse-grained AZ31 and (b) fine-grained AZ31.

$$\dot{\varepsilon} = A \left(\frac{Gb}{kT} \right) \left(\frac{\sigma - \sigma_0}{G} \right)^n \left(\frac{b}{d} \right)^p D \qquad (2)$$

where $\dot{\varepsilon}$ is the strain rate of the matrix, A is a constant, k is the Boltzmann's constant, T is the temperature, G is the shear modulus, b is the Burgers vector, d is the grain size, σ is the flow stress, σ_0 is the threshold stress, n is the stress exponent ($n = 1/m$: m is the strain rate sensitivity exponent), p is the grain size exponent and D is the diffusion coefficient. Sherby and Wadsworth suggested an effective diffusion coefficient, D_{eff}, for the analysis of superplastic flow. The effective diffusion coefficient was described by the combination of grain boundary diffusion coefficient, D_{gb}, and lattice diffusion coefficient, D_{L}, as follows:[24,25]

$$D_{\text{eff}} = D_{\text{L}} + x \left(\frac{\pi}{d} \right) \delta D_{\text{gb}}, \qquad (3)$$

where δ is the grain boundary with approximated as $2b$ and x is an unknown constant. Recently, Watanabe et al.[26,27] have proposed that the term x is estimated to be 1.7×10^{-2} for superplasticity in magnesium alloys.

The relationship between $(\dot{\varepsilon}/D_{\text{eff}})(kT/Gb)(d/b)^2$ and $(\sigma - \sigma_0)/G$ for the present materials was shown in Fig. 3, where D_{eff} is taken to be $[D_{\text{L}} + (1.7 \times 10^{-2})(\pi\delta/d)D_{\text{gb}}]$. It also included the data for superplastic behavior in magnesium alloys.[16,27–33] The superplastic behavior in the present materials was represented by a single straight line with a slope of 2, which means the strain rate sensitivity exponent $m = 2$, in the normalized plotted. In addition, it was clearly observed that two AZ31 alloys used in this study behaved identically to other superplastic magnesium alloys. Therefore, superplastic constitutive equation in magnesium alloys was given as the following equation,
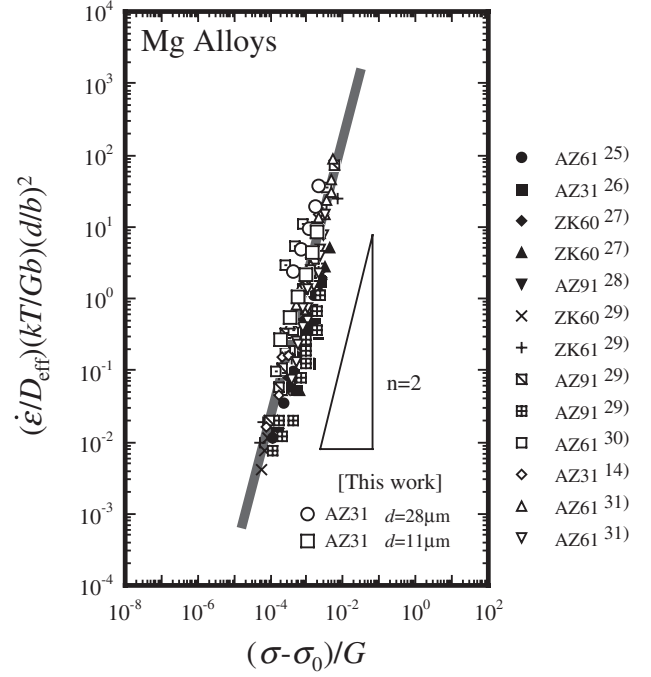

Fig. 3 The relationship between $(\dot{\varepsilon}/D_{\text{eff}})(kT/Gb)(d/b)^2$ and $(\sigma - \sigma_0)/G$ for AZ31 in the superplastic region. The figure also includes the data for superplastic behavior in magnesium alloys.[16,27–33]

$$\dot{\varepsilon} = 1.8 \times 10^6 \left(\frac{Gb}{kT} \right) \left(\frac{\sigma - \sigma_0}{G} \right)^2 \left(\frac{b}{d} \right)^2 D_{\text{eff}}. \qquad (4)$$

3.2 Diffusion bonding

The typical appearance of the diffusion bonded specimens were shown in Fig. 4 for (a) 3 h and (b) 1 h at the bonding pressure of 5 MPa on coarse-grained material. From the outside of the diffusion bonded specimen, it was very difficult to evaluate whether the diffusion bonding quality was good or not.

Using eq. (1), the results of all compressive lap shear tests after diffusion bonding test were listed in Table 2; (a) fine-
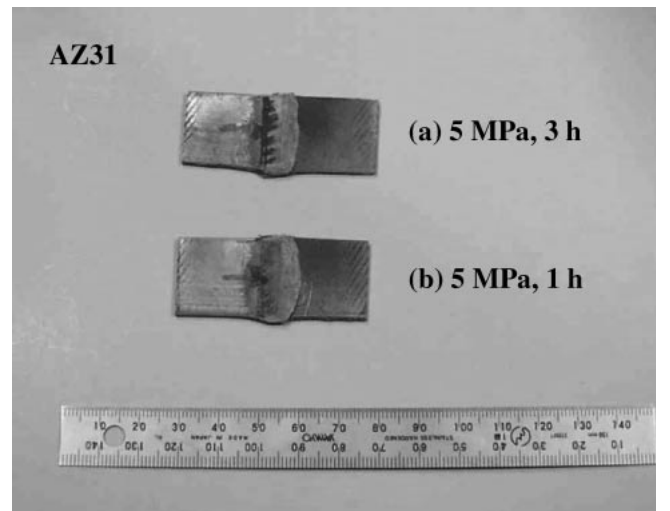

Fig. 4 Typical diffusion bonded specimen at a temperature of 673 K for (a) 3 h and (b) 1 h at 5 MPa on coarse-grained material.

Table 2 Summary of lap shear tests of diffusion bonding specimens for (a) fine-grained AZ31 and (b) coarse-grained AZ31. NA; The strength was not determined because of the specimens peeled away as soon as compression lap shear tests begin.

(a)

Bonding condition		Lap shear strength,			τ_b/τ_p (%)
Pressure, P/MPa	Time, t/h		τ_b/MPa		
	1.0	NA			NA
2.0	2.0	60.1	65.5	60.7	0.69
	3.0	64.8	66.3	63.3	0.72
	5.0	70.9	70.2	76.3	0.84
	0.5	NA			NA
3.0	1.0	71.2	72.5	64.2	0.77
	2.0	81.9	81.4	85.1	0.92
5.0	0.5	60.0	56.4	72.6	0.70
	1.0	74.8	70.5	84.2	0.85
7.0	0.5	72.0	73.1	73.6	0.81

(b)

Bonding condition		Lap shear strength,			τ_b/τ_p (%)
Pressure, P/MPa	Time, t/h		τ_b/MPa		
	3.0	NA			NA
3.0	5.0	60.4	62.5	61.5	0.72
	10	80.5	75.3	56.8	0.83
	1.0	NA			NA
5.0	2.0	58.0	56.7	51.8	0.65
	3.0	74.9	74.5	81.1	0.90
	0.5	NA			NA
7.0	1.0	59.2	54.2	55.7	0.66
	2.0	77.9	70.6	74.3	0.87
10	0.5	NA			NA
	1.0	63.8	65.5	75.6	0.81

Fig. 5 The schematic illustration of (a) void growth and (b) diffusion bonding.

grained material and (b) coarse-grained material. The maximum ratio of lap shear strength, τ_b/τ_p, were 0.90 (coarse-grained) and 0.92 (fine-grained). These conditions were obtained at a bonding pressure of 5 MPa for 3 h (coarse-grained) and 3 MPa for 2 h (fine-grained), respectively. The bonding strength depended on the pressure and time, that is, it increased as bonding time and pressure increase. It was suggested that diffusion bonding could be performed under the conditions, which were obtained superplastic behavior, in employing wrought magnesium alloys.

On the other hand, when the ratio of lap shear strength, τ_b/τ_p, was less than 0.6, the specimens peeled away as soon as the measurement of compression lap shear tests began. It was considered that diffusion bonding strength was very poor under the condition of $\tau_b/\tau_p < 0.6$. In this case, it would be required more bonding times and pressures to attain high quality in diffuison bonding.

3.3 Comparison experimental result with conventional diffusion bonding model

There are many factors such as temperature, pressure and time affecting in high quality diffusion bonding. In case of the application of SPF and DB, the bonding temperature could be taken in the superplastic temperature range. However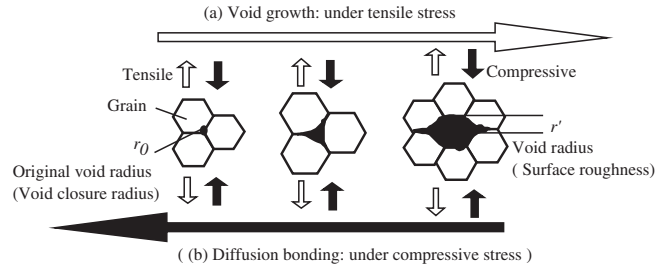, it has been very difficult to obtain its optimal bonding pressure and time in experimental. Therefore, it is necessary to develop the theoretical diffusion bonding model to predict these optimal conditions, such as pressure and time. To date, a number of theoretical models have been developed to achieve them.[34–37] All existing models on diffusion bonding considered the interfacial void shrinkage. Some void shrinkage models were developed from powder sintering models.[34] The others models were derived from void growth model under tensile creep treating void shrinkage as negative void growth.[35–37] Since many researchers have investigated void growth mechanisms of superplastic materials,[38,39] they were applied to the theoretical diffusion bonding models. The illustration of the relationship between void growth mechanism and diffusion bonding was shown in Fig. 5; (a) void growth (right-hand arrow) and (b) diffusion bonding (left-hand arrow). In general, the void would grow under tensile stress at elevated temperatures. This process was schematically illustrated in Fig. 5(a) as a right-hand arrow. However, under the compressive stress as in the diffusion bonding, the void would vanish as indicated by left-hand arrow in Fig. 5(b).

There are two models for void growth; one is plastic controlled process and the other is diffusional controlled process.[37,40,41] If the void growth is plastic controlled process, the rate of change in void radius with strain is given by[40]

$$\left(\frac{dr}{d\varepsilon}\right)_{pl} = \frac{\eta}{3}\left(r - \frac{3\gamma}{2\sigma}\right) \quad (5)$$

where r is the void radius, γ is the surface energy and η is the void growth rate parameter. It is reported that the parameter, η, is dependent on both the deformation mechanism of the matrix and the geometry of tensile deformation.[42] If the void growth is diffusional controlled process, the rate of change in the void radius with strain can be expressed as[37,41]

$$\left(\frac{dr}{d\varepsilon}\right)_{diff} = \left(\frac{2\Omega\delta D_{gb}}{kT}\right)\left(\frac{1}{r^2}\right)\left(\frac{1}{\dot{\varepsilon}_{creep}}\right)\left(\sigma - \frac{2\gamma}{r}\right) \quad (6)$$

where Ω is the atomic volume, δ is the grain boundary width, D_{gb} is the coefficient for grain boundary diffusion, and $\dot{\varepsilon}_{creep}$ is the power law equation, which is eq. (2) and typical deformation behavior of the matrix.

The variation in void growth rate, $dr/d\varepsilon$, as a function of void radius was shown in Fig. 6. The predicted void growth behavior was given by the shaded curve in Fig. 6. In Fig. 6, r_0 is the closure void radius, r' is the void radius after straining, r_c is the intersection radius of diffusional controlled
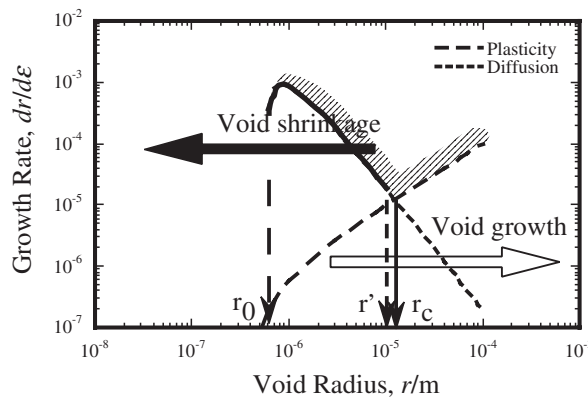
Fig. 6 The relationship between the void growth rate, $dr/d\varepsilon$, and void radius by plasticity- and diffusional-controlled processes.

Fig. 7 The relationship between the treated surface roughness, r, and the intersection radius, r_c. [7,9,11-13,16,17,20,43]

process and plastic controlled process. The approximate value of the intersection radius, r_c, is obtained by equating eqs. (5) and (6).

$$r_c \approx \left(\frac{2\Omega\delta D_{gb}}{kT}\right)^{1/3}\left(\frac{\sigma}{\dot{\varepsilon}_{creep}}\right)^{1/3} \qquad (7)$$

It is reported that the faster void growth process is dominant under the tensile stress.[38] The void grows up to r_c by diffusional controlled process, and thereafter by plastic controlled process with strain. However, during diffusion bonding, the void shrinkage proceeds in the opposite direction compared with void growth process. In case of diffusion bonding, the void radius, r', corresponds to the surface roughness. In general, the surface is blasted or polished in order to enhance the bonding quality before diffusion bonding.[11-13,18,20,36] Therefore, it is supposed that these treatments bring about rugged surface equal to the value of r'. From Fig. 6, it is well noted that the void vanishes by plastic controlled process up to r_c, and thereafter by diffusional controlled process to r_0. Even if the treated surface roughness is less than the intersection radius, $r' < r_c$, the void shrinkage proceeds only by diffusional controlled process.

The relationship between treated surface roughness and intersection radius was shown in Fig. 7 by using eq. (7) and superplastic titanium alloys[7,9,11,12] and superplastic aluminum alloys.[13,20,43] The necessary factors to calculate were listed in Table 3.[44,45] This figure also included the data for superplastic AZ31 magnesium alloys.[17] In previous diffusion bonding using superplastic titanium alloys and super-
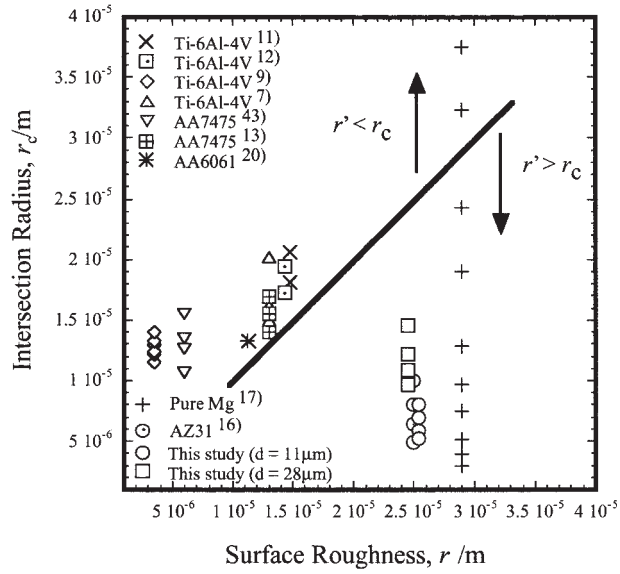
plastic aluminum alloys, it was found that the value of surface roughness, r', was smaller than the value of intersection radius, r_c. Therefore, the previous diffusion bonding models were developed by considering only diffusional controlled process as a void shrinkage mechanism. In order to compare these theoretical model with experimental results, many researchers tested diffusion bonding in experimental. It was reported that the experimental bonding times were agreed with prediction analysis for these superplastic materials.[7,11-13] However, the comparison of experimental result by using superplastic magnesium alloys and the previous theoretical models took place in previous report.[16] The values of previous diffusion bonding models were not in good agreement with experimental results, that is to say, theoretical values were larger than experimental values. This disagreement resulted from that not only the diffusional controlled process but also the different void shrinkage process, which is plastic controlled process, would occur.[16] From Fig. 7, it was apparent that the surface roughness was larger than the intersection radius at superplastic magnesium alloys. In case of high depression resistance materials such as magnesium,[2] it is difficult not only to bring a fine surface roughness but also to apply to previous diffusion bonding models.

Table 3 Parameters to obtain high quality diffusion bonding conditions.[44,45]

	Mg	Al	Ti
Atomic volume, Ω/m³	2.33×10^{-28}	1.66×10^{-29}	1.76×10^{-29}
Burger's vector, b/m	3.21×10^{-10}	2.86×10^{-10}	2.95×10^{-10}
Surface energy, γ/Jm⁻²	5.6×10^{-1}	9.0×10^{-1}	***
Grain boundary width, δ/m	6.42×10^{-10}	5.72×10^{-10}	5.90×10^{-10}
Grain boundary diffusion, D_{gb}/m²s⁻¹	$7.8 \times 10^{-3} \exp(-Q/RT)$	$8.7 \times 10^{-5} \exp(-Q/RT)$	$6.1 \times 10^{-7} \exp(-Q/RT)$
Activation energy, Q/kJmol⁻¹	92	84	97

3.4 New theoretical diffusion bonding model and its application to predict bonding conditions

Based on the above analyses, it is apparent that the diffusion bonding model should include two void shrinkage processes of both diffusional controlled process and plastic controlled process in order to estimate the optimal diffusion bonding conditions. It is suggested that the optimal diffusion bonding time, t, to obtain high quality joining is corresponding to the void closure time, where r' becomes r_0. Equations (5) and (6) would be rewritten as functions of void radius and the time:

$$\left(\frac{dr}{dt}\right)_{pl} = \frac{\eta \dot{\varepsilon}_{creep}}{3}\left(r - \frac{3\gamma}{2\sigma}\right) \tag{8}$$

and

$$\left(\frac{dr}{dt}\right)_{diff} = \frac{2\Omega\delta D_{gb}}{kT}\left(\frac{1}{r^2}\right)\left(\sigma - \frac{2\gamma}{r}\right). \tag{9}$$

The optimal diffusion bonding time, t, is the sum of integral of eqs. (8) and (9):

$$t = \left(\frac{dr}{dt}\right)_{diff} + \left(\frac{dr}{dt}\right)_{pl} = \int_0^t dt = \frac{kT}{2\eta\Omega\delta D_{gb}}\int_{r_0}^{r_c}\left[\frac{r^3}{r\sigma - 2\gamma}\right]dr + \int_{r_c}^{r'}\left[\frac{2\sigma}{2r\dot{\varepsilon}_{creep}\sigma - 3\gamma\dot{\varepsilon}_{creep}}\right]dr. \tag{10}$$

The integral limits are $r = r'$ at $t = 0$ and $r = r_0$ when the void closure. Depending on the surface roughness and intersection radius following two equations can be obtained.

$$t_{r_c > r'} = \frac{kT}{2\Omega\delta D_{gb}\sigma}\left[\frac{1}{3}(r_c^3 - r_0^3) + \frac{\gamma}{\sigma}(r_c^2 - r_0^2) + \frac{4\gamma^2}{\sigma^2}(r_c - r_0) + \frac{8\gamma^3}{\sigma^3}\left\{\log\left|\frac{r_c\sigma - 2\gamma}{r_0\sigma - 2\gamma}\right|\right\}\right] \tag{11}$$

$$t_{r_c < r'} = \frac{kT}{2\Omega\delta D_{gb}\sigma}\left[\frac{1}{3}(r_c^3 - r_0^3) + \frac{\gamma}{\sigma}(r_c^2 - r_0^2) + \frac{4\gamma^2}{\sigma^2}(r_c - r_0) + \frac{8\gamma^3}{\sigma^3}\left\{\log\left|\frac{r_c\sigma - 2\gamma}{r_0\sigma - 2\gamma}\right|\right\}\right] + \frac{1}{\dot{\varepsilon}}\log\left|\frac{2r'\dot{\varepsilon}\sigma - 3\gamma\dot{\varepsilon}}{2r_c\dot{\varepsilon}\sigma - 3\gamma\dot{\varepsilon}}\right| \tag{12}$$

By using eqs. (4) and (7), in order to estimate the theoretical diffusion bonding model whether eq. (11) or eq. (12), the variation at applied stress as a function of the intersection radius at the temperature of 673 K was shown in Fig. 8 for (a) fine-grained material and (b) coarse-grained material. The necessary factors to calculate the relationship were listed in Table 3.[44,45] From Fig. 8, it is found that the intersection radius depends on applied stress and grain size; intersection radius decreases as increased applied stress increases and/or refined grain size. When the treated surface roughness is smaller than the intersection radius, the void shrinkage process is only diffusional controlled (Region I). Therefore, the diffusion bonding time, t, to obtain optimal
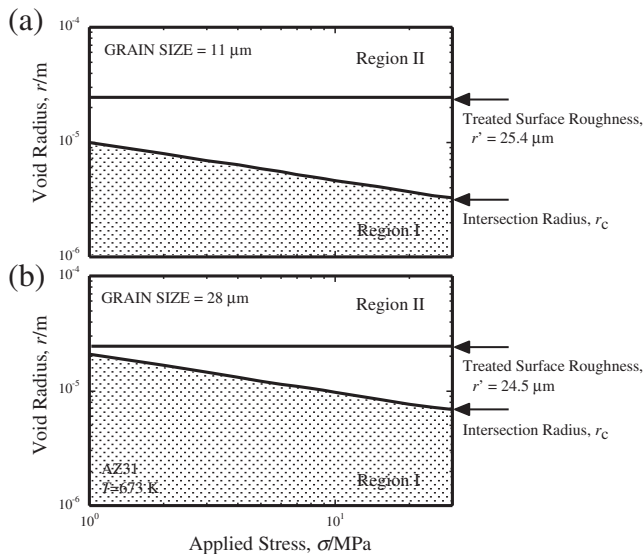

Fig. 8 The variation at applied stress as a function of the intersection radius at temperature of 673 K in superplastic AZ31 magnesium alloys for (a) fine-grained material and (b) coarse-grained material.

diffusion bonding conditions could be used in only diffusional controlled process in eq. (11) as well as conventional models. However, when the treated surface roughness is larger than the intersection radius, the void shrinkage is both diffusional controlled process and plastic controlled process (Region II). Therefore, new theoretical diffusion bonding, equation is expressed as eq. (12) including both diffusional controlled process and plasticity controlled process. In this study, since all testing conditions exist in Region II, eq. (12) is used in order to calculate optimal diffusion bonding condition.

The experimental bonding time to obtain high values in lap shear strength in our study was compared with those of prediction analysis by present diffusion bonding model. The variation in bonding time as a function of applied stress predicted from eqs. (4) and (12) was shown in Fig. 9 for (a) fine-grained material and (b) coarse-grained material. The symbols of $\bigcirc$, $\triangle$ and $\times$ in Fig. 9 showed $\tau_b/\tau_p \geq 0.80$, $0.80 > \tau_b/\tau_p \geq 0.60$ and $\tau_b/\tau_p < 0.60$, respectively. It was easy to predict the bonding time to obtain high quality joining. The bonding time also depended on the bonding pressure. The experimental bonding time corresponded to the results by the prediction analysis in considering both diffusional controlled process and plastic controlled process. By comparison with Fig. 9, the material with fine grained could be achieved optimal condition, $0.8 > \tau_b/\tau_p$, much faster than that with coarse grained at a constant bonding pressure. This is due to the superplastic behavior depending on the grain size. Since these testing conditions could be obtained superplastic behavior, the grain boundary sliding would be occurred in case of diffusion bonding as well as superplasticity.

Figure 9 also included the prediction bonding time by Chen-Argon[35] and Pilling-Ridely models.[36] The comparisons among the present diffusion bonding model, Chen-Argon model and Pilling-Ridely model showed that the
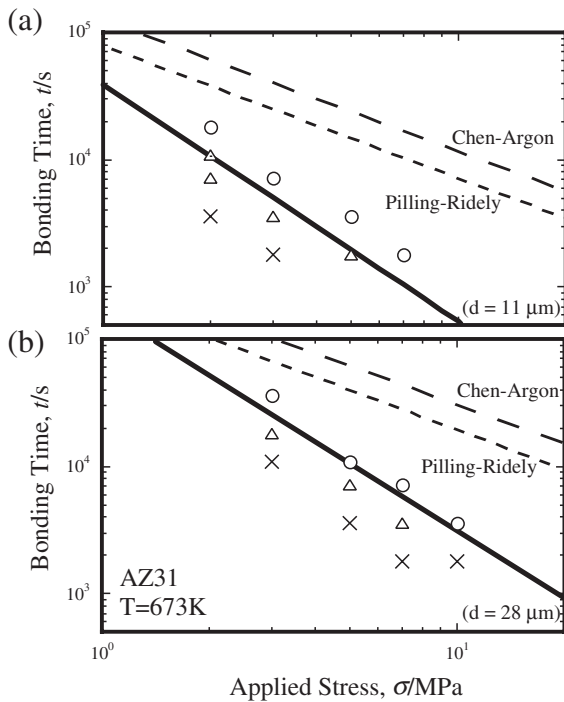
(a)

(b)

Fig. 9 Comparison between the experimental bonding time and the bonding times by prediction analysis, which are Chen-Argon, Pilling-Ridely and present models, for (a) fine-grained material and (b) coarse-grained material. The solid line is present model, and the dish line are previous models. ○: $\tau_b/\tau_p \geq 0.8$, △: $0.8 > \tau_b/\tau_p \geq 0.6$, ×: $0.6 < \tau_b/\tau_p$.

prediction bonding times by present model were shorter than that of both prediction analyses. This is because the previous diffusion bonding models do not include the plastic controlled process. The void growth/vanish rate in plastic controlled process is faster than that in the diffusional flow process. In case of large treated surface roughness, it is important to discuss the relationship between treated surface roughness and intersection radius by using eq. (7). On the other hand, in the comparison with between treated surface roughness and intersection radius, new theoretical diffusion bonding model could predict the optimal diffusion bonding condition in case of large surface roughness on not only magnesium alloys but also other materials such as titanium, aluminum, iron alloys. Therefore, it is proposed that new diffusion bonding model could be applicable for the wider surface-finished conditions on materials.

In order to describe the effect of grain size more distinct, the variation in bonding time as a function of grain size was shown in Fig. 10 at several bonding pressures. From Fig. 10, it is found that the optimal bonding time decreases with grain refinement. Therefore, in order to obtain bonding time reduction, it is important to develop fine-grained materials. Figure 10 is the prediction map for high-quality diffusion bonding on superplastic magnesium alloys.

4.　Summary

The superplastic characteristic and diffusion bonding behavior was investigated in commercial wrought AZ31 magnesium alloy having grain sizes with two different of 11 and 28 μm. The following results were obtained.
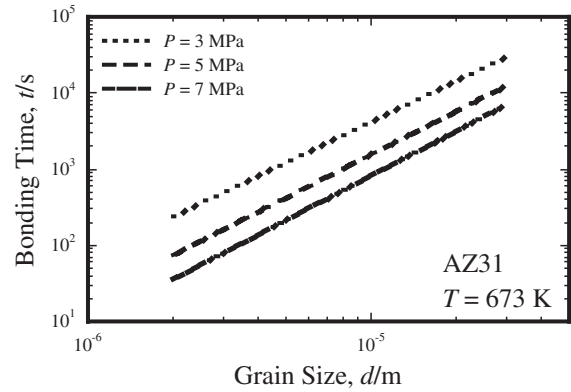

Fig. 10 The prediction map in high quality diffusion bonding on superplastic magnesium alloys by using theoretical analysis.

(1) From strain rate change tests, both materials behaved in a superplastic manner in the low strain rate range at the temperature of 673 K.
(2) The constitutive for superplastic flow equation was developed form the normalized plotted. Both materials were in good agreement with other superplastic magnesium alloys.
(3) From the diffusion bonding tests at 673 K, several optimal conditions were obtained. The maximum ratio of lap shear strength was 0.90 (coarse-grained material) and 0.92 (fine-grained material) at a bonding pressure of 5 and 3 MPa, with bonding time of 3 and 2 h, respectively.
(4) We suggested the diffusion bonding model including both diffusional controlled process and plastic controlled process. Theoretical prediction for attaining good bonding condition was in good agreement with experimental results.
(5) The material with fine grained AZ31 could be achieved optimal diffusion bonding conditions much faster than that with coarse grained AZ31. This was related to the fact that the superplastic behavior was grain size dependent phenomena.
(6) Using the theoretical diffusion bonding model and experimental results, the prediction map for high quality diffusion bonding on superplastic magnesium alloys clarified.

Acknowledgments

REFERENCES

1) S. Kamado and Y. Kojima: Materia Japan **38** (1999) 285–290.
2) ASM Specialty Handbook, *Magnesium and magnesium alloys*, (Materials Park, OH, ASM International. 1999)
3) T. Mukai, H. Watanabe and K. Higashi: Mater. Sci. Tech. **16** (2000) 1314–1319.
4) M. T. Salehi, J. Pilling, N. Ridley and D. L. Hamilton: Mater. Sci. Eng. **A150** (1992) 1–6.
5) J. R. Williamson: *Superplastic Forming of Structural Alloys*, ed. N. E. Paton and C. H. Hamilton, (TMS-AIME, Warrendale, Pennsylvania, 1982) pp. 291–306.
6) J. R. Williamson: *Superplastic in Aerospace*, ed. C. Heikkenen and T. R. McNelly, (TMS-AIME, Warrendale, Pennsylvania, 1988) pp. 315–330.
7) J. Pilling: Mater. Sci. Eng. **A100** (1988) 137–144.
8) O. Ohashi: Kinzoku **56** (1986) 14–20.
9) K. Iizumi, A. Ogawa and N. Suzuki: J. Jpn. Inst. Light Metals **49** (1999) 368–372.
10) G. Cam, H. Clemens, R. Gerling and M. Kocak: Z. Metallk. **90** (1999) 284–288.
11) M. F. Islam, J. Pilling and N. Ridley: Mater. Sci. Tech. **13** (1997) 1045–1050.
12) M. T. Salehi, J. Pilling, N. Ridley and D. L. Hamilton: Mater. Sci. Eng. **A150** (1992) 1–6.
13) J. Pilling and N. Ridley: Mater. Sci. Tech. **3** (1987) 353–359.
14) N. Ridley, J. Pilling, A. Tekin and Z. W. Guo: *Diffusion Bonding*, ed. by R. Pearce (Cranfield School of Industrial Science, 1987) pp. 129–142.
15) T. D. Byun and P. Yavari: *Superplasticity in Aerospace-Aluminium*, ed. by R. Pearce and L. Kelly, (Cranfield, 1985) pp. 285–294.
16) H. Somekawa, H. Hosokawa, H. Watanabe and K. Higashi: Mater. Sci. Eng. **A339** (2003) 328–333.
17) H. Somekawa, H. Hosokawa, H. Watanabe and K. Higashi: Mater. Trans. **42** (2001) 2075–2079.
18) N. Ridley, M. T. Salehi and J. Pilling: Mater. Sci. Tech. **8** (1992) 791–795.
19) M. F. Islam and N. Ridley: Scr. Mater **38** (1998) 1187–1193.
20) A. S. Zuuzi, H. Li and G. Dong: Mater. Sci. Eng. **A270** (1999) 244–248.
21) T. G. Langdon: Metall. Trans. **13A** (1982) 689–701.
22) O. D. Sherby and J. Wadsworth: Prog. Mater. Sci. **33** (1989) 169–221.
23) R. S. Mishra, T. R. Bieler and A. K. Mukherjee: Acta Metall. **43** (1995) 877–891.
24) O. D. Sherby and J. Wadsworth: *Development and Characterization of Fine-Grain Superplastic Materials*, (American Society for Metals, Metals Park, OH, 1982) pp. 355.
25) P. Metenier, G. Gonzalez-Doncel, O. A. Ruano, J. Wolfenstine and O. D. Sherby: Mater. Sci. Eng. **A125** (1990) 195–202.
26) H. Watanabe, T. Mukai, M. Kohzu, S. Tanabe and K. Higashi: Mater. Trans., JIM **40** (1999) 809–814.
27) H. Watanabe, T. Mukai, M. Kohzu, S. Tanabe and K. Higashi: Acta Metall. **47** (1999) 3753–3758.
28) H. Watanabe, T. Mukai, K. Ishikawa, Y. Okanda, M. Kohzu and K. Higashi: J. Japan Ins. Light Metals **49** (1999) 401–404.
29) H. Watanabe, T. Mukai and K. Higashi: Scr. Mater. **40** (1999) 477–484.
30) M. Mabuchi, K. Kubota and K. Higashi: Mater. Trans., JIM **36** (1995) 1249–1254.
31) M. Mabuchi, T. Asahina, H. Iwasaki and K. Higashi: Mater. Sci. Tech. **13** (1999) 825–831.
32) H. Tsutsui, H. Watanabe, T. Mukai, M. Kohzu, S. Tanabe and K. Higashi: Mater. Trans., JIM **40** (1999) 931–934.
33) W. J. Kim, S. W. Chung, C. S. Chung and D. Kum: Acta Metall. **49** (2001) 3337–3345.
34) B. Derby and E. R. Wallach: Met. Sci. **16** (1982) 49–56.
35) I. W. Chen and A. S. Argon: Acta Metall. **29** (1981) 1759–1768.
36) J. Pilling, D. W. Livesey, J. B. Hawkyard and N. Ridley: Met. Sci. **18** (1984) 117–122.
37) W. Beere and M. V. Speight: Met. Sci. **12** (1978) 172–176.
38) A. H. Chokshi and T. G. Langdon: Acta Metall. **35** (1987) 1089–1101.
39) H. Iwasaki, M. Mabuchi and K. Higashi: Acta Metall. **49** (2001) 2269–2275.
40) J. W. Hancock: Metal. Sci. **10** (1976) 319–325.
41) M. V. Speight and W. Beere: Metal. Sci. **9** (1975) 190–191.
42) A. C. F. Cocks and M. F. Ashby: Met. Sci. **16** (1982) 465–474.
43) M. Hiroyashi, Y. T. Park and H. Asanuma: J. Jpn. Inst. Light Metals **41** (1991) 687–692.
44) E. Robinowitz: *Friction and wear of materials*, (J. Wiltey and Sones, 1965).
45) H. J. Frost and M. F. Ashby: *Deformation-mechanism Maps*, (Pergamon Press, Oxford, 1982) pp. 44.